Use of shear-wave elastography to distinguish complex and complicated fibroadenomas from simple fibroadenomas

Işıl Başara Akın
Hakan Özgül
Canan Altay
Mustafa Seçil
Merih Güray Durak
Duygu Gürel
Pınar Balcı

PURPOSE

Simple fibroadenomas (SFAs), complex fibroadenomas (CFAs), and cellular fibroadenomas (CeFAs) are variants of fibroadenomas. Additionally, some degenerative, hyperplastic, and metaplastic changes may occur in fibroadenomas, forming complicated fibroadenomas. Distinctive ultrasonography (US) features in variants of fibroadenomas and complicated fibroadenomas have not been reported. Shear-wave elastography (SWE) can be applied to effectively discriminate between these variants and complicated fibroadenomas. In this study, we aimed to evaluate SWE findings to discriminate between SFAs and other variants.

METHODS

In total, 48 patients (26 with SFAs, 16 with CFAs, 3 with CeFAs, and 3 with complicated fibroadenomas) participated in this study. The lesions were classified into two groups according to histopathologic diagnoses. The SWE evaluation and lesion elasticity scores (E_{max}, E_{mean}, and E_{min}) were both assessed in m/s and k/Pa, respectively. Two observers measured E_{max}, E_{mean}, and E_{min}. Brightness (B)-mode US findings based on the Breast Imaging Reporting and Data System categorization and elasticity scores were recorded. In the statistical analyses, the chi-square test and non-parametric tests were performed. Fisher's exact test was used to compare independent groups, and Spearman's correlation coefficients were used to correlate the SWE data between the two observers. Additionally, receiver operating characteristic curves were analyzed to evaluate the diagnostic performance of the elasticity values.

RESULTS

The B-mode US features in both groups showed no statistical significance. The set of SWE values of both observers demonstrated strong statistical significance in discriminating between group 1 (SFAs) and Group 2 (CFAs, CeFAs, and complicated fibroadenomas).

CONCLUSION

As the fibroadenoma variants and complicated fibroadenomas have similar US findings, SWE in addition to a conventional B-mode examination can increase the diagnostic performance to discriminate SFAs from other complex and complicated forms of fibroadenomas.

KEYWORDS

Cellular fibroadenoma, complex fibroadenoma, complicated fibroadenoma, shearwave elastography, simple fibroadenoma, ultrasonography

The English in this document has been checked by at least two professional editors, both native speakers of English.
For a certificate, please see

http://www.textcheck.com/certificate/J96xm9

From the Department of Radiology (I.B.A. ✉ slbasara@yahoo.com, C.A., M.S., P.B.), Dokuz Eylül University Faculty of Medicine, İzmir, Turkey; Department of Pathology (M.G.D., D.G.), Dokuz Eylül University Faculty of Medicine, İzmir Turkey; Clinic of Radiology (H.O.), Kemalpaşa State Hospital, İzmir, Turkey.

Fibroadenomas are common benign breast lesions, particularly in young and adolescent female patients.[1] Of all the benign breast lesions, 50%–60% are fibroadenomas; when biopsied, 40% are diagnosed as fibroadenomas.[2,3]

Simple fibroadenomas (SFAs) consist of epithelial and stromal histologic components.[4] Fibroadenomas are classified according to their histopathologic components and features,[5] and complex fibroadenomas (CFAs) and cellular fibroadenomas (CeFAs) are two other variants.[5-7] Of all fibroadenomas, 22% are diagnosed as CFAs based on histopathologic evaluation. The rate of development of invasive breast cancer is 3.1 times higher in patients with CFAs than in the normal population. In particular, perilesional benign proliferative changes and a family history of breast cancer increase the risk of malignancy in patients with SFAs and/or CFAs.[8]

CeFAs are characterized by uniform stromal cellularity without stromal atypia, but the diagnosis can be challenging based on histopathologic evaluation because the histopathologic features usually overlap with benign phyllodes tumors.[9]

Degenerative changes, such as hyperplastic changes, squamous metaplasia, focal tubular adenoma, myoid metaplasia, myxoid degeneration, cystic changes, adipose differentiation, infarction, and osteochondroid metaplasia, may occur in fibroadenomas.[6,10,11] In addition, intraductal papillomas, including fibroadenomas, have been reported in the literature.[12] These fibroadenomas are different from the other variants and can be defined as complicated fibroadenomas. If the hyperplasia behaves similarly in normal breast tissue, the risk of developing malignancy can increase within these complicated fibroadenomas.[13]

Main points

- Ultrasonography (US) findings in fibroadenoma variants and complicated fibroadenomas are similar; distinctive US features for each entity have not been reported. Although they have similar US features, clinical evaluations and approaches differ for simple fibroadenomas (SFAs), other variants, and complicated fibroadenomas.

- As brightness-mode US does not have specific distinctive features, unnecessary surgeries and interventional procedures may occur.

- Additional US imaging methods such as shear-wave elastography can assist in discrimination between SFAs, other variants, and complicated fibroadenomas.

Ultrasonography (US) is the main diagnostic method, and lesions are evaluated according to the Breast Imaging Reporting and Data System (BI-RADS).[14] Fibroadenoma variants and complicated fibroadenomas with suspicious US characteristics are categorized as BI-RADS 4, and exact diagnoses are obtained after histopathologic evaluation. Although US findings in fibroadenoma variants and complicated fibroadenomas tend to be similar, distinctive US features for each entity have not been reported in the literature.[14] Although they have similar US features, clinical evaluations and approaches differ for SFAs, other variants, and complicated fibroadenomas.[15,16] For SFAs, follow-up at appropriate intervals is required. For CFAs and complicated fibroadenomas that are suspicious lesions, surgical excision with safe margins is recommended for treatment. Surgery also enables an accurate diagnosis of CeFAs.[1,17,18]

Additional US imaging methods such as shear-wave elastography (SWE) can assist with discrimination between SFAs, other variants, and complicated fibroadenomas. SWE is a quantitative method involving the application of an acoustic radiation force pulse sequence for shear-wave propagation.[19] Tissue stiffness affects quantitative values according to the rapidity of sound changes,[19] with malignant tissues having stiffer components and exhibiting higher velocities than benign areas.[19] These SWE features facilitate discrimination between benign and malignant lesions.[20] In addition, SWE is a useful imaging modality for differentiating benign lesions from those with a low risk of malignancy, which have indistinct brightness (B)-mode US characteristics and the same suspicious BI-RADS features.[21-23]

Although fibroadenomas are benign lesions, they may exhibit suspicious B-mode US features.[15,16] Additional imaging modalities, including SWE, may increase the diagnostic performance of conventional B-mode US.[23] Only one case series in the literature has specifically described the SWE features of CFAs.[7] To the best of our knowledge, no study has specifically evaluated the SWE findings of fibroadenoma variants. In this study, we evaluated the utility of additional SWE findings for differentiating between SFAs and other variants.

Methods

Patients

This retrospective study was approved by our Institutional Review Board, and the requirement for informed consent was waived. The non-interventional ethics committee approval protocol number was 7005-GOA,

and the decision number was 2022/13-18. Patients diagnosed with SFAs, CFAs, CeFAs, or complicated fibroadenomas between January 2019 and December 2021 were included in the study. Patients with optimal B-mode US-SWE images and completed histopathologic evaluations were included in the study, whereas patients with artifactual images were not. Additionally, for an optimal histopathologic result evaluation, patients who underwent surgery in another medical center were excluded from the study. A total of 48 patients were reviewed. The patients were divided into groups 1 and 2. Patients with SFAs were classified into group 1, and patients with CFAs, CeFAs, and complicated fibroadenomas formed group 2. B-mode US and SWE images from the picture archiving and communication system (PACS) were evaluated. Lesion sizes, B-mode US findings according to BI-RADS categorization, and elasticity scores were recorded.

Histopathologic diagnosis and evaluation

Most of the lesions were diagnosed using core and/or excisional biopsy. In group 1, 10 lesions were diagnosed through core biopsy and 16 through excisional biopsy. In group 2, 5 lesions (CFAs) were diagnosed using core biopsy, and excisional biopsies were performed on 14 lesions (11 CFAs and 3 complicated fibroadenomas). One CeFA was diagnosed through direct excisional biopsy, and two were diagnosed as phyllodes tumors and one as a juvenile fibroadenoma after core biopsies. In the three CeFAs diagnosed through core biopsies, exact diagnoses were subsequently made after excisional biopsies. In the core biopsies, a 14-Gauge core needle was used. All biopsies were performed under US guidance. In each biopsy session, at least five tissue samples were extracted.

Wire-guided excisional biopsies were performed for non-palpable lesions. The diagnostic method was determined according to the patient's medical condition and preference as well as the surgeon's decision. Patients with SFAs were followed up with after diagnosis. For lesions diagnosed as CFAs or CeFAs via core biopsies, excision with tumor bed resection was performed after the core biopsy.

B-mode US evaluation

The US examinations were performed using an ML6–15 MHz linear transducer (LOGIQ S8; GE Healthcare, Milwaukee, WI, USA). All the relevant images were archived in the Sectra IDS7 PACS system (Sectra AB, Linköping, Sweden) for further evaluation.

The US examinations were performed by 3 different radiologists with 30, 17, and 6 years of breast imaging experience. All the lesions stored in the PACS system were evaluated by two radiologists with 17 and 6 years of breast imaging experience. The B-mode features were determined by consensus between the two radiologists.

The largest diameter of each lesion was measured, and general B-mode US characteristics were evaluated and recorded according to the Fifth Edition of BI-RADS US features. These features included shape (round, oval, or irregular), orientation (parallel or non-parallel), margin (circumscribed, non-circumscribed, indistinct, angular, microlobulated, or spiculated), echo pattern (hyperechoic, hypoechoic, isoechoic, or complex cystic/heterogeneous), and posterior acoustic features (no posterior acoustic features, enhancement, shadowing, or a combination of features). The lesions were then classified according to BI-RADS as follows: BI-RADS 3–probably benign; BI-RADS 4A–low suspicion of malignancy; BI-RADS 4B–intermediate suspicion of malignancy; and BI-RADS 4C–moderate suspicion of malignancy.[24]

Additional imaging evaluation

The patients were evaluated using the additional imaging methods of mammography (MG), tomosynthesis (TS) and magnetic resonance imaging (MRI). The MG and TS examinations were conducted using a MG device (Selenia, Hologic, Bedford, MA, USA). As standard, in MG, each case had four images [right–left craniocaudal and left–right mediolateral oblique (MLO)]. If required, additional positions were also obtained. Digital breast TS was conducted in MLO positions in standard modalities. The MG and TS examinations were applied to patients of appropriate ages. In all these patients, B-mode US examinations were conducted.

The MRI examinations were realized using two different 1.5 T MRI devices: 1. Intera software (version 8.1; Philips Medical Systems, Eindhoven, The Netherlands), 2. Gyroscan Achieva, (Philips, ACS-NT, Bothell, WA, USA). Phased-array breast coils were applied in the prone position. The conventional sequences were as follows: precontrast axial turbo spin echo (TSE) T1-weighted (T1W) [3-mm slice thickness, 3.3 spacing, matrix: 512 × 512, field of view (FOV): 40, repetition time (TR): 516 ms, echo time (TE): 80 ms, echo train length (ETL): 4], axial fat-saturated (SPIR) TSE T2-weighted (3-mm slice thickness, 3

spacing, matrix: 512 × 512, FOV: 40, TR: 6,700 ms, TE: 120 ms, ETL: 30), after contrast material administration (intravenously, 0.1–0.2 mmol/kg), axial dynamic gradient echo, T1W high-resolution isotropic volume examination (2-mm slice thickness, 1 spacing, matrix: 480 × 480, FOV: 40, TR: 50,000 ms, TE: 2,500 ms, ETL: 40), and late postcontrast phase, axial TSE, SPIR T1W (3-mm slice thickness, 3.3 spacing, matrix: 512 × 512, FOV: 42, TR: 550 ms, TE: 80 ms, ETL: 4). The MRI examinations were applied to the patients who had suspicious US and/or MG–TS findings to identify solutions.

SWE evaluation

The elastography features were analyzed after the B-mode US evaluation using a 9L linear transducer (LOGIQ S8; GE Healthcare). All three investigators had been trained by GE Healthcare and subsequently performed at least 20 SWE examinations under their supervision. The most important aspect of the SWE examination is avoiding probe compression to prevent pseudo stiffness. In addition, to prevent motion artifacts, the patients are asked to hold their breath and remain still during the SWE examination, if required.

In the SWE evaluation, the lesions were located within the central part of "elasticity boxes," which were as remote as possible from skin and muscle tissues (unless these tissues exhibited lesion involvement). During the examination, the probe was applied as lightly as possible to prevent pressure on the lesion. The elastography image acquisition time was approximately 10–20 s, and a shear-wave color map was obtained. The colors ranged from dark blue to red, corresponding to the lowest and highest degree of stiffness, respectively. Both B-mode US and additional SWE examinations were performed before histopathologic evaluations.

The regions of interest (ROIs) were placed on the most inelastic areas of the lesions according to the shear-wave color map. The maximum dimensions of the ROI were 3 × 3 mm. Elasticity values [E_{max}, E_{mean}, E_{min}, and standard deviation (SD)] were obtained in m/s and k/Pa. All measurements were made and recorded by radiologists with 17 and 6 years of breast imaging experience, working independently. Both radiologists were blinded to the histopathologic diagnoses of the lesions.

Statistical analysis

The patients' ages, largest lesion diameters, histopathologic diagnoses, B-mode US imaging findings, and final BI-RADS categori-

zations were recorded. All statistical analyses were performed using Statistical Package for the Social Sciences version 24.0 software.

The chi-square test was performed to evaluate categorical variables, and Fisher's exact test was used to compare independent groups. Non-parametric tests were used for further group analyses. The Kruskal–Wallis test was used to evaluate continuous data, which are presented as mean ± SD. The patients' ages and lesion dimensions were compared between the two groups using the non-parametric Mann–Whitney U test. The mean elasticity values were evaluated through the t-test, and Spearman's correlation coefficients were used to correlate SWE data between the two observers. Receiver operating characteristic curves were analyzed to evaluate the diagnostic performance of the elasticity values. The Youden index was used to define the optimal cut-off value, and cut-off values were then calculated in terms of sensitivity and specificity. The sensitivity, specificity, positive predictive value (PPV), and negative predictive value (NPV) of the cut-off values were measured. Statistical significance was defined as $P < 0.050$.

Results

Patients

A total of 48 patients were included in this study, of whom 26 (54.2%), diagnosed with SFAs, were assigned to group 1. Group 2 comprised 22 (45.8%) patients, including 12 and 7 with diagnoses of CFAs and CeFAs, respectively. Another three patients were diagnosed with complicated fibroadenomas (one each with intraductal papilloma, chondroid metaplasia, and myoid metaplasia).

The median (minimum–maximum) age was 47.3 (24–68) years in group 1 and 42.09 (24–65) years in group 2. There was no statistical difference in age between the groups (P = 0.722).

The median (minimum–maximum) diameters of the lesions in groups 1 and 2 were 14.03 (5–30) and 19.04 (9–50) mm, respectively. There was no statistical significance between the groups (P = 0.130).

B-mode US findings

The distributions of the B-mode US features of the lesions in both groups are presented in Table 1. There was no statistical significance between the groups. The P value of the echo pattern was 0.063. Although the

P value was >0.050, all patients (n = 5) with a complex cystic echo pattern were included in Group 2.

The BI-RADS classification distribution is shown in Table 2; no statistical significance was identified between the two groups in terms of the BI-RADS classification (*P* = 0.783).

Additional imaging findings

Nineteen patients in Group 1 and 14 patients in Group 2 were evaluated using MG–TS. In Group 2, 13 patients had a well-defined nodular lesion, the lesion in 1 patient was an irregular contoured lesion, and 5 patients had no findings from the MG–TS examinations. In Group 2, well-defined nodular lesions were identified in eight patients, and four had no findings.

MRI was performed on 13 patients in Group 1 and on 9 patients in Group 2. In Group 1, no enhancement was observed in two lesions in two patients. All the lesions exhibited enhancement without washout, and in two lesions, slight enhancement was observed. In Group 2, all the lesions had late phase enhancement with no washout, and five lesions were enhanced slightly. Hypointense linear septa were determined in nine patients (five in Group 1 and four in Group 2).

SWE findings

Lesion elasticity was evaluated in terms of both m/s and k/Pa. The elasticity values of E_{max}, E_{mean}, and E_{min} were obtained by two ob-
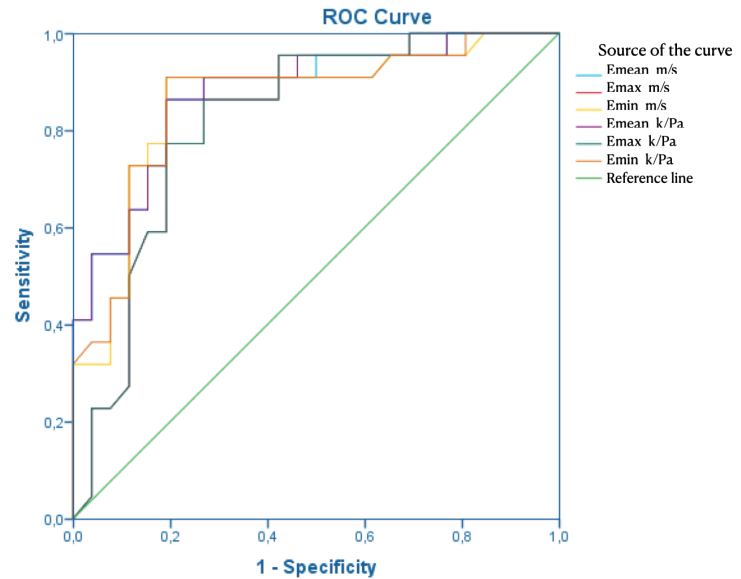

Figure 1. Receiver operating characteristic curves of the elasticity (E_{max}, E_{mean} and E_{min}) values (in both m/s and k/Pa).

Table 1. Distribution of grayscale ultrasonography features in all groups

Grayscale US features			Group 1 (n - %)	Group 2 (n - %)	*P*
Shape	Oval		16 - (61.5%)	10 - (45.4%)	
	Round		7 - (27%)	10 - (45.4%)	0.408
	Irregular		3 - (11.5%)	2 - (9.2%)	
Orientation	Parallel		16 - (61.5%)	13 - (59.1%)	
	Non-parallel		10 - (38.5%)	9 - (40.9%)	0.863
Margin	Circumscribed		6 - (23.2%)	5 - (22.7%)	
	Non-circumscribed	Indistinct	1- (3.8%)	0	
		Angular	13 - (50%)	9 - (41%)	
		Microlobulated	5 - (19.2%)	7 - (31.8%)	0.767
		Spiculated	1 - (3.8%)	1 - (4.5%)	
Echo pattern	Hypoechoic		16 - (61.5%)	14 - (41%)	
	Hyperechoic		1 - (3.8%)	0	
	Isoechoic		0	1 - (4.5%)	
	Heterogenous		9 - (34.7%)	7 - (31.8%)	0.063
	Complex cystic-heterogeneous		0	5 - (22.7%)	
Posterior acoustic features	No posterior acoustic features		12 - (41.2%)	16 - (72.3%)	
	Enhancement		6 - (23.1%)	1 - (4.5%)	
	Shadowing		5 - (19.2%)	1 - (4.5%)	0.083
	Combined		3 - (11.5%)	4 - (18.2%)	

n, number of patients; US, ultrasonography.

Table 2. Breast Imaging Reporting and Data System classification distribution

BI-RADS classification	BI-RADS 3	BI-RADS 4A	BI-RADS 4B	BI-RADS 4C	*P*
Group 1 (n - %)	3 - (11.5%)	17 - (65.4%)	4 - (15.4%)	2 - (7.7%)	
Group 2 (n - %)	1 - (4.5%)	14 - (63.6%)	5 - (22.7%)	2 - (9.2%)	0.783

n, number of patients; BI-RADS, Breast Imaging Reporting and Data System.

Table 3. Mean elasticity values and P values of both observers' measurements

		Observer 1	Observer 2	*P*
E_{max}	Group 1	5.4573 ± 2.10657 m/s 102.1231 ± 71.41531 k/Pa	5.7354 ± 1.77669 m/s 107.8373 ± 58.36010 k/Pa	
	Group 2	7.8745 ± 1.32761 m/s 190.8886 ± 58.69822 k/Pa	7.8455 ± 1.30104 m/s 189.4809 ± 57.34698 k/Pa	
E_{mean}	Group 1	4.6096 ± 1.78241 m/s 72.6350 ± 48.21512 k/Pa	4.9742 ± 1.59203 m/s 80.0615 ± 45.99172 k/Pa	<0.001
	Group 2	7.0182 ± 1.21245 m/s 151.9655 ± 46.19820 k/Pa	6.8927 ± 1.25090 m/s 146.3909 ± 47.49218 k/Pa	
E_{min}	Group 1	3.6438 ± 1.47768 m/s 46.1835 ± 35.88449 k/Pa	3.7519 ± 1.32861 m/s 46.8531 ± 32.56780 k/Pa	
	Group 2	5.8005 ± 1.31117 m/s 107.0027 ± 42.16296 k/Pa	5.7614 ± 1.37844 m/s 104.7450 ± 42.85316 k/Pa	

E, elasticity.

servers, significantly differentiating between Groups 1 (SFAs) and 2 (CFAs, CeFAs, and complicated fibroadenomas) (all *P* values were <0.001). All data, including the elasticity values and *P* values for the measurements of both observers, are presented in Table 3.

The Spearman's correlation coefficients of the elasticity values (in both m/s and k/Pa), obtained by the two observers, exhibited high compatibility (*P* < 0.001). All the Spearman's correlation coefficient values are shown in Table 4.

Receiver operating characteristic curves were obtained for the E_{max}, E_{mean}, and E_{min} values (in both m/s and k/Pa) (Figure 1). When the cut-off value for E_{max} to discriminate between Groups 1 and 2 was 6.41 m/s, the sensitivity, specificity, PPV, NPV, and area under the curve (AUC) were 86.4%, 80.8%,

72%, 82.6%, and 0.820, respectively. A cut-off value of 131.02 k/Pa for E_{max} produced sensitivity, specificity, PPV, NPV, and AUC values of 81.8%, 73.1%, 69.2%, 81.8%, and 0.820, re-

spectively. A cut-off value of 5.79 m/s for E_{mean} revealed sensitivity, specificity, PPV, NPV, and AUC values of 86.4%, 80.8%, 72%, 82.6%, and 0.874, respectively. When the cut-off value

Table 4. Spearman's correlation coefficient values and *P* values of both observers' measurements

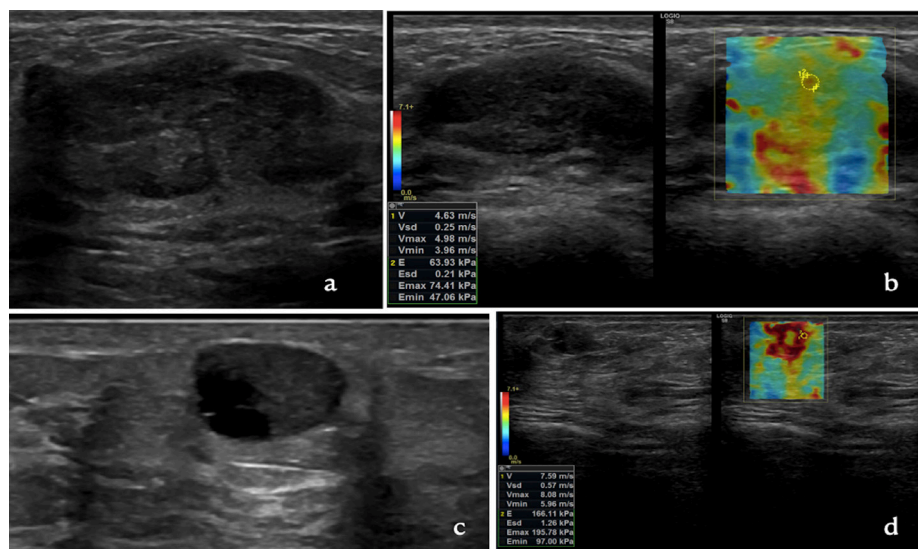|	m/s	kPa	*P*
E_{max}	0.958	0.959	<0.001
E_{mean}	0.970	0.974	<0.001
E_{min}	0.967	0.966	<0.001

E, elasticity.

Figure 2. (a) Brightness (B)-mode an ultrasonography (US) image of a 42-year-old female patient with a palpable lesion on her left breast showing an oval-shaped solid breast lesion with indistinct contours and heterogeneous echogenicity. **(b)** Shear-wave elastography (SWE) examination reveals a predominantly green and yellow pattern. Maximum elasticity scores are 4.98 m/s or 74.41 kPa. The lesion was defined as Breast Imaging Reporting and Data System (BI-RADS) 4A, and core needle biopsy was applied. The lesion was diagnosed as a simple fibroadenoma. **(c)** A 46-year-old female patient. In the B-mode US image, the lesion is well-defined with a circumscribed margin. The echo pattern of the lesion is complex cystic. **(d)** In the SWE examination, the lesion has stiffer features with a predominantly red pattern. Maximum elasticity scores were 8.08 m/s or 195.78 kPa. According to these imaging features, the lesion was categorized as BI-RADS 4A. An excisional biopsy was performed at the request of the patient, and the diagnosis was complex fibroadenoma.

Table 5. Distribution of sensitivity, specificity, PPV, NPV, and AUC according to the cut-off values of E_{max}, E_{mean}, and E_{min}

	Cut-off	Sensitivity (%)	Specificity (%)	PPV (%)	NPV (%)	AUC	*P*
E_{max}	6.41 m/s	86.4%	80.8%	72%	82.6%	0.820	0.065
	131.02 k/Pa	81.8%	73.1%	69.2%	81.8%	0.820	0.142
E_{mean}	5.79 m/s	86.4%	80.8%	72 %	82.6%	0.874	0.052
	99.87 k/Pa	86.4%	80.8%	72%	82.6%	0.876	0.064
E_{min}	4.61 m/s	90.9%	80.8%	76%	76%	0.858	0.024
	63.2 k/Pa	90.9%	80.8%	76%	86.9%	0.860	0.015

E, elasticity; PPV, positive predictive value; NPV, negative predictive value; AUC, area under the curve.
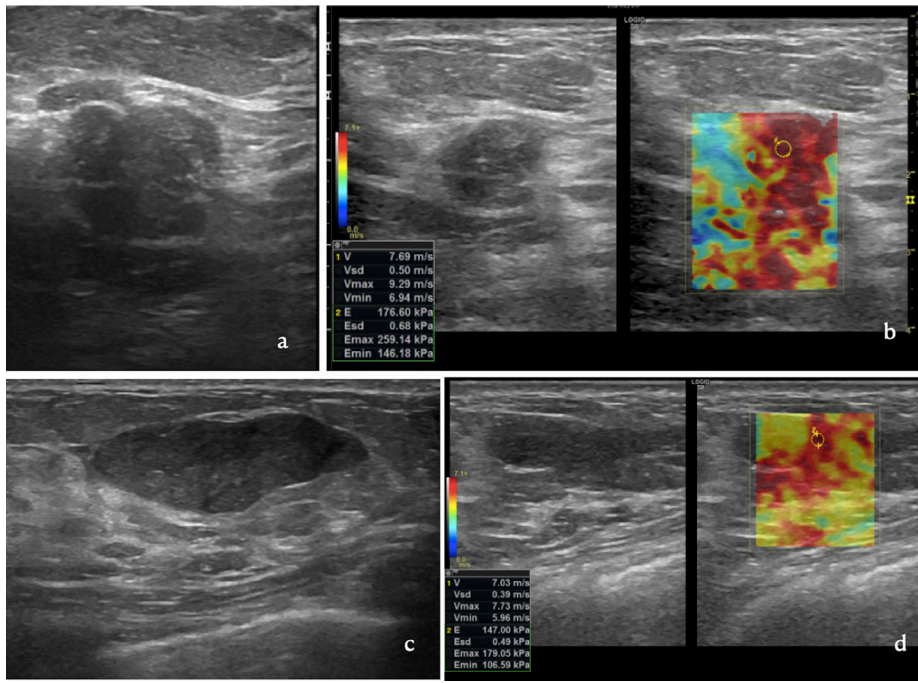
Figure 3. (a) Brightness (B)-mode ultrasonography (US) image of a 51-year-old female patient showing a round, well-defined solid lesion with minimal heterogeneous echo pattern. The orientation of the lesion is vertical. **(b)** The shear-wave elastography (SWE) image shows a predominantly red heterogeneous pattern compatible with a stiff lesion. The maximum elasticity scores are 9.29 m/s or 259.14 kPa. As a result of the combination of the B-mode and SWE findings, the lesion was categorized as Breast Imaging Reporting and Data System (BI-RADS) 4A. The lesion was diagnosed as fibroadenoma including intraductal papilloma after excisional biopsy. **(c)** A 36-year-old female patient with a growing palpable left breast lesion. In the B-mode US image, the lesion is homogeneous hypoechoic. The shape of the lesion is oval with a circumscribed contour and parallel orientation. **(d)** The SWE examination revealed a predominantly red pattern. The lesion was defined as a stiff lesion with maximum elasticity scores of 7.73 m/s or 179.05 kPa. The lesion was classified as BI-RADS 4A through both imaging and clinical findings. The lesion was excised and diagnosed as cellular fibroadenoma.

of E_{mean} was 99.87 k/Pa, the sensitivity, specificity, PPV, NPV, and AUC were 86.4%, 80.8%, 72%, 82.6%, and 0.876, respectively. A cut-off value of 4.61 m/s for E_{min} had sensitivity, specificity, PPV, NPV, and AUC values of 90.9%, 80.8%, 76%, 86.9%, and 0.858, respectively. When the cut-off value of E_{min} was 63.2 k/Pa, the sensitivity, specificity, PPV, NPV, and AUC values were 90.9%, 80.8%, 76%, 86.9%, and 0.860, respectively (Table 5; Figures 2 and 3).

Discussion

This study demonstrated that the addition of SWE to conventional B-mode imaging facilitates the differentiation of SFAs from complex and complicated fibroadenomas. This is significant because B-mode imaging findings in fibroadenomas with suspicious B-mode US features do not discriminate SFAs from suspicious forms or variants. There are pronounced differences in the treatment, follow-up procedures, and potential risk of malignancy between SFAs and other variants;[16] therefore, interventions should be tailored precisely to the diagnosis for optimal patient management.[14] Additional SWE findings enhance the diagnostic performance of B-mode US findings.

The mean age in Group 1 was 47.3 years (range: 24–68 years), whereas in Group 2, it was 42.09 years (range: 24–65 years). The mean age did not significantly differ between the two groups, although the patients in Group 1 were older. Most of the patients in Group 2 were diagnosed with CFAs, and their age distribution was similar to that in the literature. In a study by Pinto et al.[15], the age distribution of patients with SFAs and CFAs was similar to that in our study.[16] However, in another study, patients with CFAs were older than those with SFAs, which was considered to be related to the transformation of complex characteristics with older age.[19] In our study, the younger age of Group 2 patients was related to heterogeneous diagnoses, which included CeFAs and complicated fibroadenomas. Edwards et al.[9] reported that the age of the patients with CeFAs in their study was 35.2–32.7 years. Notably, our institution is a tertiary hospital for breast imaging and treatment, and patients are referred regardless of age.

In this study, the mean diameter of the lesions was smaller in Group 1 (14.03 ± 7.3 mm) than in Group 2 (19.04 ± 11.4 mm), although this was not statistically significant. This is consistent with the literature.[15,17] The smaller mean diameter in Group 1 in our study was attributed to the older age of this group because SFAs decrease in size and regress with age.[15] The larger diameters of the Group 2 lesions were attributed to the transformation of the complex characteristics of fibroadenomas.[19]

In our study, the B-mode US features did not differentiate between the two groups. Most of the lesions in Group 1 were oval. In Group 2, there were equal numbers of oval and round lesions. However, no statistical significance was identified between the two groups in lesion shape, which is consistent with the literature.[15,17] Although there were more lesions with non-circumscribed than circumscribed contours in both groups, the difference was non-significant, which is contrary to the literature.[15] The lesions included in this study were all nominated for histopathologic evaluations according to the BI-RADS categorization. We did not evaluate the SFAs without any changes during the follow-up period, which we believe accounted for the majority of the non-circumscribed lesions. The orientation and posterior acoustic characteristics were not statistically significant between the two groups. In both groups, most lesions were in a parallel orientation, as is reported in the literature.[15] The lesions in our study typically exhibited no posterior acoustic features. Five lesions in Group 2 had a complex cystic echo pattern, which was not detected in any Group 1 lesions. In the studies by Basara Akin et al.[7] and Pinto et al.[15], a complex cystic echo pattern was identified significantly more frequently than any other pattern in CFAs; we attribute this echo pattern to the histopathologic features of CFAs.[8] None of the lesions in either of our groups had parenchymal calcifications.

In our study, 19 patients in Group 1 and 14 in Group 2 were evaluated using MG and TS. In all these images, no specific imaging findings discriminated the groups from each other. The major imaging finding was well-defined nodular lesions. Additionally, MRI was performed in 13 patients in Group 1 and 9 in Group 2. In both groups, the main MRI findings were diffuse enhancement without washout, hypointense linear septa in the lesions, and enhancement in the le-

sions. The ages in each group were similar, and consequently, the menopausal statuses of the patients revealed no differences. Additionally, no specific difference was detected in risk factors. All these imaging findings and demographic features were insufficient to provide a prominent contribution to the diagnoses and prevent unnecessary interventional procedures. The SWE features were the main features that discriminated between the two groups. All the lesions in both groups were benign. In clinical practice, US is the main imaging modality for evaluating solid breast lesions; although benign, they are generally classified as BI-RADS 4.[25] While BI-RADS 4 lesions are suspicious for malignancy, the actual rate of malignancy varies between 3% and 94%. These lesions are diagnosed through either core biopsy or surgical excision, and SFAs should be followed up with appropriate procedures.[17] As CFAs have an increased risk of malignancy, particularly when accompanied by peripheral hyperplastic changes, surgical excision with large and clean surgical margins is recommended for optimal treatment.[17] All CeFAs are challenging to treat. Histopathologic evaluations of core biopsy materials in CeFAs have revealed variations in stroma composition along with glands with a high cellular content.[9] This makes it difficult to distinguish between CeFAs, other fibroadenoma variants, and phyllodes tumors in histopathologic evaluations.[9,26] There are no guidelines for the management and follow-up of CeFAs.[9] The surgical excision of biopsy-proven CeFAs is a logical treatment option for an accurate diagnosis and can also inform follow-up treatment. In the literature, few studies exist on complicated fibroadenomas. Although data regarding these lesions are limited, the increased risk of malignant transformation of such lesions with hyperplastic contents is the most concerning aspect. As the optimal follow-up procedure is unclear, surgical excision is the recommended treatment option.

In the literature, various studies have discussed the diagnostic performance of additional SWE findings for differentiating malignant and benign breast lesions and for evaluating fibroepithelial lesions, including fibroadenomas.[2,23,27-31] Two studies have evaluated the contribution of SWE findings to the diagnosis of fibroadenomas.[2,29] Evans et al.[2] evaluated both B-mode US and SWE features for diagnosing fibroadenomas in the absence of biopsy, concluding that, because clinically benign solid breast lesions with benign B-mode US and SWE findings exhibited no malignant transformation, biopsy and follow-up procedures were unnecessary. In a study of 700 symptomatic breast lesions, none of the lesions were cancerous according to B-mode US and SWE examinations.[32] Another study examined whether SWE and color Doppler US findings could prevent the unnecessary surgical excision of fibroepithelial lesions, including SFAs and phyllodes tumors diagnosed through core biopsies.[29] Lower E_{mean} and E_{max} values were obtained for SFAs than for phyllodes tumors.[29] In the literature, a combination of B-mode US and SWE features has been evaluated to differentiate between SFAs and phyllodes tumors. In our study, different fibroadenoma variants and forms were evaluated, revealing that B-mode US features were ineffective for differentiating SFAs from forms with higher malignant transformation potential. A cut-off E_{min} value of 63.2 k/Pa demonstrated higher sensitivity (90.9%), specificity (80.8%), PPV (76%), and NPV (86.9%) values than all other cut-off values.

Combining SWE and conventional US imaging findings is useful for evaluating, and potentially downgrading or upgrading, BI-RADS 3–4A lesions.[23] A multinational study of 939 breast lesions by Berg et al.[23] revealed that combining SWE features with BI-RADS characteristics improved the specificity and accuracy of the diagnoses. In our study, although all the lesions were benign, additional SWE findings made a major contribution to the differentiation of SFAs from other forms. In our patients, the application of MG and/or TS did not make any difference in the downgrading or upgrading of BI-RADS classifications. The MRI findings were all evaluated using a combination of other imaging modality findings, specifically, B-mode US and SWE findings. Although enhancement patterns had generally unsuspicious features, enhancing lesions with suspicious US and SWE findings were upgraded and histopathologic evaluations were performed.

Our study has several limitations. First and most importantly, the number of patients was limited. In addition, particularly in Group 2, patients were not homogeneous in terms of diagnoses. By increasing the number of patients in both groups and the diagnostic homogeneity of Group 2, SWE findings could be more discriminative. Second, we evaluated quantitative SWE characteristics. In another study, qualitative SWE features, including lesion shape and the homogeneity of elasticity within lesions and surrounding tissue, were evaluated in addition to quantitative features. SWE images were also obtained, and lesion diameter, perimeter, and area were measured. Furthermore, diameter ratios and mass areas on B-mode and SWE images were calculated. These measurements increased the specificity.[23] Adding qualitative elastography features to B-mode and quantitative elastography findings may significantly increase diagnostic performance in larger patient series. As a final limitation, our study was retrospective, only evaluating lesions with known pathologic diagnoses. A prospective study including follow-up could validate our results.

In conclusion, adding SWE to conventional B-mode examinations can increase the ability to differentiate SFAs from more CFAs. To the best of our knowledge, this is the only study to evaluate additional SWE features to diagnose suspicious fibroadenomas. A classification of BI-RADS 4, particularly the BI-RADS 4A subdivision, is associated with low malignancy rates. Although SFAs are benign, for a final diagnosis, interventional methods are required in suspicious cases. Combining non-invasive SWE and B-mode US examinations facilitates discrimination between SFAs, CFAs, and CeFAs. Finally, SWE may be useful for optimizing the diagnosis of fibroadenomas and avoiding unnecessary biopsies, which can cause confusion and anxiety in patients.

Conflict of interest disclosure

The authors declared no conflicts of interest.

References

1. Basara Akin I, Balci P. Fibroadenomas: a multidisciplinary review of the variants. *Clin Imaging*. 2021;71:83-100. [CrossRef]

2. Evans A, Sim YT, Lawson B, Whelehan P. Audit of eliminating biopsy for presumed fibroadenomas with benign ultrasound greyscale and shear-wave elastography findings in women aged 25-39 years. *Clin Radiol*. 2020;75(11):880.e1-880.e3. [CrossRef]

3. Greenberg R, Skornick Y, Kaplan O. Management of breast fibroadenomas. *J Gen Intern Med*. 1998;13(9):640-645. [CrossRef]

4. Hanby AM, Millican-Slater R, Dessauvagie. Fibroepithelial neoplasms of the breast. *Diagnostic Histopathology*. 2017;23(4):149-158. [CrossRef]

5. Humphrey PA, Dehner LP, Pfeifer JD. The Washington Manual of Surgical Pathology. 1st ed. Lippincott Williams & Wilkins; 2008:262. [CrossRef]

6. Kuijper A, Mommers EC, van der Wall E, van Diest PJ. Histopathology of fibroadenoma of

the breast. *Am J Clin Pathol*. 2001;115(5):736-742. [CrossRef]

7. Basara Akin I, Ozgul HA, Guray Durak M, Balci P. Evaluation of elastographic features in complex fibroadenomas with radiologic-pathologic correlation. *J Ultrasound Med*. 2021;40(8):1709-1718. [CrossRef]

8. Dupont WD, Page DL, Parl FF, et al. Long-term risk of breast cancer in women with fibroadenoma. *N Engl J Med*. 1994;331(1):10-15. [CrossRef]

9. Edwards T, Jaffer S, Szabo JR, Sonnenblick EB, Margolies LR. Cellular fibroadenoma on Core needle biopsy: management recommendations for the radiologist. *Clin Imaging*. 2016;40(4):587-590. [CrossRef]

10. Rosen PP. Fibroepithelial neoplasms. In: Rosen PP, eds. Rosen's Breast Pathology. 3rd ed. Philadelphia: Lippincott Williams & Wilkins; 2009;87-201. [CrossRef]

11. Durak MG, Karaman I, Canda T, Balci P, Harmancioğlu O. Cystic fibroadenoma of the breast: a case report. *Turk Patoloji Derg*. 2011;27(3):254-256. [CrossRef]

12. Cummings MC, da Silva L, Papadimos DJ, Lakhani SR. Fibroadenoma and intraduct papilloma--a common pathogenesis? *Virchows Arch*. 2009;455(3):271-275. [CrossRef]

13. Dupont WD, Page DL. Risk factors for breast cancer in women with proliferative breast disease. *N Engl J Med*. 1985;312(3):146-151. [CrossRef]

14. Raza S, Goldkamp AL, Chikarmane SA, Birdwell RL. US of breast masses categorized as BI-RADS 3, 4, and 5: pictorial review of factors influencing clinical management. *Radiographics*. 2010;30(5):1199-1213. [CrossRef]

15. Pinto J, Aguiar AT, Duarte H, Vilaverde F, Rodrigues Â, Krug JL. Simple and complex fibroadenomas are there any distinguishing sonographic features? *J Ultrasound Med*. 2014;33(3):415-419. [CrossRef]

16. Durhan G, Önder Ö, Azizova A, et al. Can radiologist and pathologist reach the truth together in the diagnosis of benign fibroepithelial lesions? *Eur J Breast Health*. 2019;15(3):176-182. [CrossRef]

17. Basara Akin I, Ozgul H, Simsek K, Altay C, Secil M, Balci P. Texture analysis of ultrasound ımages to differentiate simple fibroadenomas from complex fibroadenomas and benign phyllodes tumors. *J Ultrasound Med*. 2020;39(10):1993-2003. [CrossRef]

18. Sklair-Levy M, Sella T, Alweiss T, Craciun I, Libson E, Mally B. Incidence and management of complex fibroadenomas. *AJR Am J Roentgenol*. 2008;190(1):214-218. [CrossRef]

19. Barr RG. Sonographic breast elastography: a primer. *J Ultrasound Med*. 2012;31(5):773-783. [CrossRef]

20. Çebi Olgun D, Korkmazer B, Kılıç F, et al. Use of shear wave elastography to differentiate benign and malignant breast lesions. *Diagn Interv Radiol*. 2014;20(3):239-244. [CrossRef]

21. Shang J, Ruan LT, Wang YY, et al. Utilizing size-based thresholds of stiffness gradient to reclassify BI-RADS category 3-4b lesions increases diagnostic performance. *Clin Radiol*. 2019;4(4):306-313. [CrossRef]

22. Wang M, Yang Z, Liu C, et al. Differential diagnosis of breast category 3 and 4 nodules through BI-RADS classification in conjunction with shear wave elastography. *Ultrasound Med Biol*. 2017;43(3):601-606. [CrossRef]

23. Berg WA, Cosgrove DO, Doré CJ, et al. Shear-wave elastography improves the specificity of breast US: the BE1 multinational study of 939 masses. *Radiology*. 2012;262(2):435-449. [CrossRef]

24. Lee KA, Talati N, Oudsema R, Steinberger S, Margolies LR. BI- RADS 3: Current and future use of probably benign. *Curr Radiol Rep*. 2018;6(2):5. [CrossRef]

25. Raza S, Chikarmane SA, Neilsen SS, Zorn LM, Birdwell RL. BI- RADS 3, 4, and 5 lesions: value of US in management--follow-up and outcome. *Radiology*. 2008;248(3):773-781. [CrossRef]

26. Jacobs TW, Chen YY, Guinee DG Jr, et al. Fibroepithelial lesions with cellular stroma on breast core needle biopsy: are there predictors of outcome on surgical excision? *Am J Clin Pathol*. 2005;124(3):342-354. [CrossRef]

27. Kim GR, Choi JS, Han BK, Ko EY, Ko ES, Hahn SY. Combination of shear-wave elastography and color Doppler: Feasible method to avoid unnecessary breast excision of fibroepithelial lesions diagnosed by core needle biopsy. *PLoS One*. 2017;12(5):e0175380. [CrossRef]

28. Tang Y, Liang M, Tao L, Deng M, Li T. Machine learning-based diagnostic evaluation of shear-wave elastography in BI-RADS category 4 breast cancer screening: a multicenter, retrospective study. *Quant Imaging Med Surg*. 2022;12(2):1223-1234. [CrossRef]

29. Yeo SH, Kim GR, Lee SH, Moon WK. Comparison of ultrasound elastography and color Doppler ultrasonography for distinguishing small triple-negative breast cancer from fibroadenoma. *J Ultrasound Med*. 2018;37(9):2135-2146. [CrossRef]

30. Park SY, Kang BJ. Combination of shear-wave elastography with ultrasonography for detection of breast cancer and reduction of unnecessary biopsies: a systematic review and meta-analysis. *Ultrasonography*. 2021;40(3):318-332. [CrossRef]

31. Shi XQ, Li JL, Wan WB, Huang Y. A set of shear wave elastography quantitative parameters combined with ultrasound BI-RADS to assess benign and malignant breast lesions. *Ultrasound Med Biol*. 2015;41(4):960-966. [CrossRef]

32. Giannotti E, Vinnicombe S, Thomson K, et al. Shear-wave elastography and greyscale assessment of palpable probably benign masses: is biopsy always required? *Br J Radiol*. 2016;89(1062):20150865. [CrossRef]